Supplemental Table I. *Rattus norvegicus* Primer Sequences

Gene	Primer Sequence (5'-3')	Accession No.
Acot2	(F) CCTACGAAACTGAGGGCTGA	NM_138907.2
	(R) GCTCAGCGTAGCATTTGTCC	
Adss	(F) CTCCCAGGATGGAACACAGA	NM_001105975.1
	(R) GCATTGCTGGCAGTCCTTAG	
Cacnb2	(F) CCACAATGAGTGCAGCAAAC	NM_053851.1
	(R) CACAGATGGTTGCAATGGAG	
Csnk1g1	(F) AAGTGGAATGTGGGTCTGGA	NM_022288.1
	(R) TGAGTCCTTCCTTCCCCAAG	
Dscr1	(F) GCCCGTTGAAAAAGCAGAAT	NM_153724
	(R) GACAGGGGGTTGCTGAAGTT	
Dusp1	(F) GAGGACAACCACAAGGCAGA	NM_053769.3
	(R) CGTCCAGCTTCACTCGGTTA	
Fam126a	(F) TGTGCTGTGGTGCTAACTGG	XM_575330.3
	(R) CCACACATGCAGCTTTCTCA	
Fzd7	(F) TGACTGTCCTCCGATTTTGC	XM_237191.5
	(R) AGCTCCAGTCAACTGATCGTG	
Gla	(F) TGTTCATGCAGATGGCAGAG	NM_001108820.1
	(R) AGCCTTTGCTGTGGACGTAA	
Hsp1a1/b	(F) GCAACGTGCTCATCTTCGAC	(a) NM_031971.2
	(R) CGCTTGTTCTGGCTGATGTC	(b) NM_212540.1
Kif5c	(F) AGACCAAGTCCACGCTGATG	NM_001107730.1
	(R) TCATCCTCAGGCACAGCTTC	
Mgat1	(F) GGGCTTGTATTCGTCCAGAA	NM_030861.1
	(R) ACAGGTCCAACTGGGTGAAG	
Mobkl2a	(F) TGGACCTGCTTATGGACTGG	NM_001108734.2
	(R) GCAGGAAGGTCTTGGGAAAC	
Otud1	(F) GAGAAGTTCAGCCTCCTGCAT	XM_574086.3
	(R) TGTTTGACCCAGCAAACCAT	
Pdlim5	(F) AGAAGAGGATCCCAGGGTGA	NM_053326.1
	(R) GGATTCGGAAGGAACGAGAC	
Procr	(F) ACCTGTCCCAGTTCAACAGC	NM_001025733.2
	(R) ACGAAGGCACTTCCATTCAC	
Rapgef2	(F) AAGGGAGTTTGGAGCGTCAT	NM_001107684.1
	(R) AGAGACTGGCACCGAGTCAA	
Rbm14	(F) CTATGCTGCACAGGCCACTA	XM_002728823.2
	(R) GCTGATGACTGAGTGCGGTA	
Rras2	(F) CAGAAACCCTTCCCAACAGA	NM_001013434.1
	(R) AAACCAGAAGCCATCCACAG	
Vegfc	(F) ATGTGGGGAAGGAGTTTGGA	NM_053653.1
	(R) GTTTGGGGCCTTGAGAGAGA	
18S	(F) CGGCTACCACATCCAAGGAA	M11188.1
	(R) AGCTGGAATTACCGCGGC	

Supplemental Table I. Designed and validated primer sequences for *in vitro* validation.

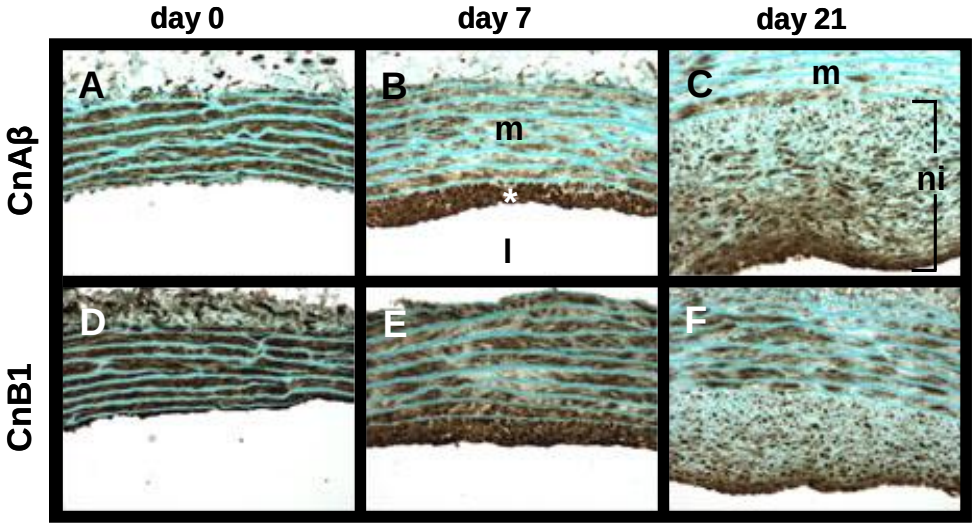

Supplemental Figure I. Immunohistochemistry reveals that both CnAβ and CnB1 are upregulated in the developing neointima (asterisk in panel B) following balloon injury of the rat thoracic aorta. Tunica media (m), neointima (ni), lumen (l).

A. PROCR-WT-luc

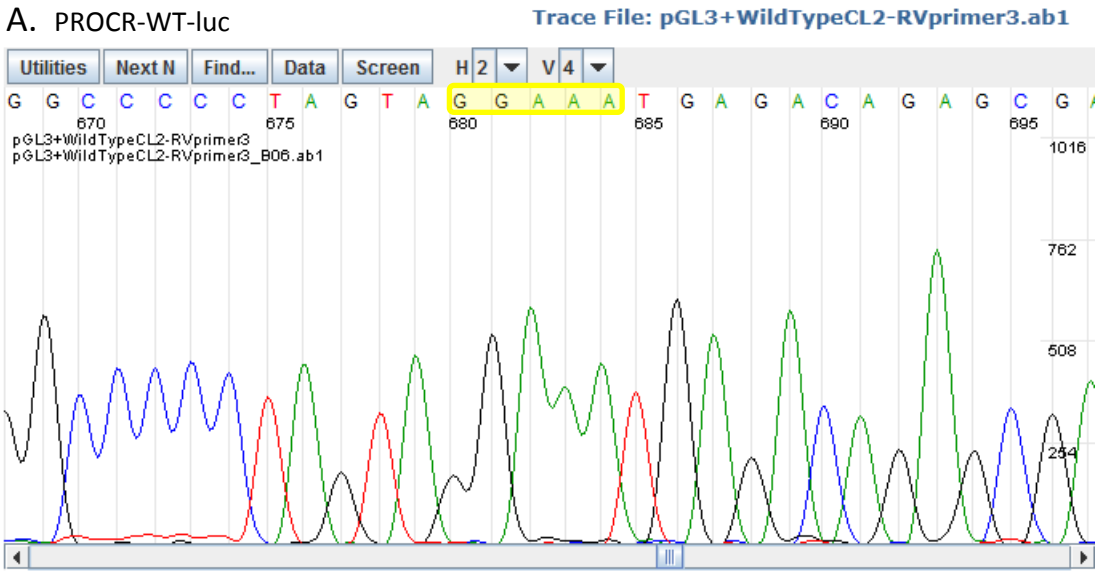

B. PROCR-MUT-luc

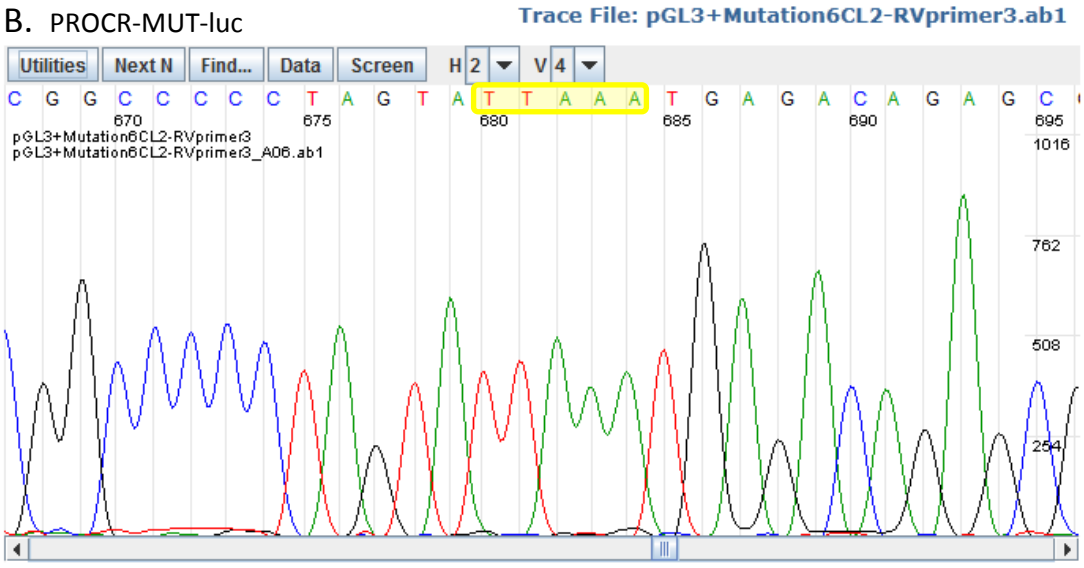

Supplemental Figure II. PROCR promoter luciferase construct sequence validations. (A) Trace files from the sequencing facility (GeneWiz) verifies inclusion of the NFAT binding motif in the PROCR-WT-luc plasmid and **(B)** successful mutation of the NFAT site (GGAAA→TTAAA) in the PROCR-MUT-luc plasmid. (NFAT sites/mutations highlighted in yellow)

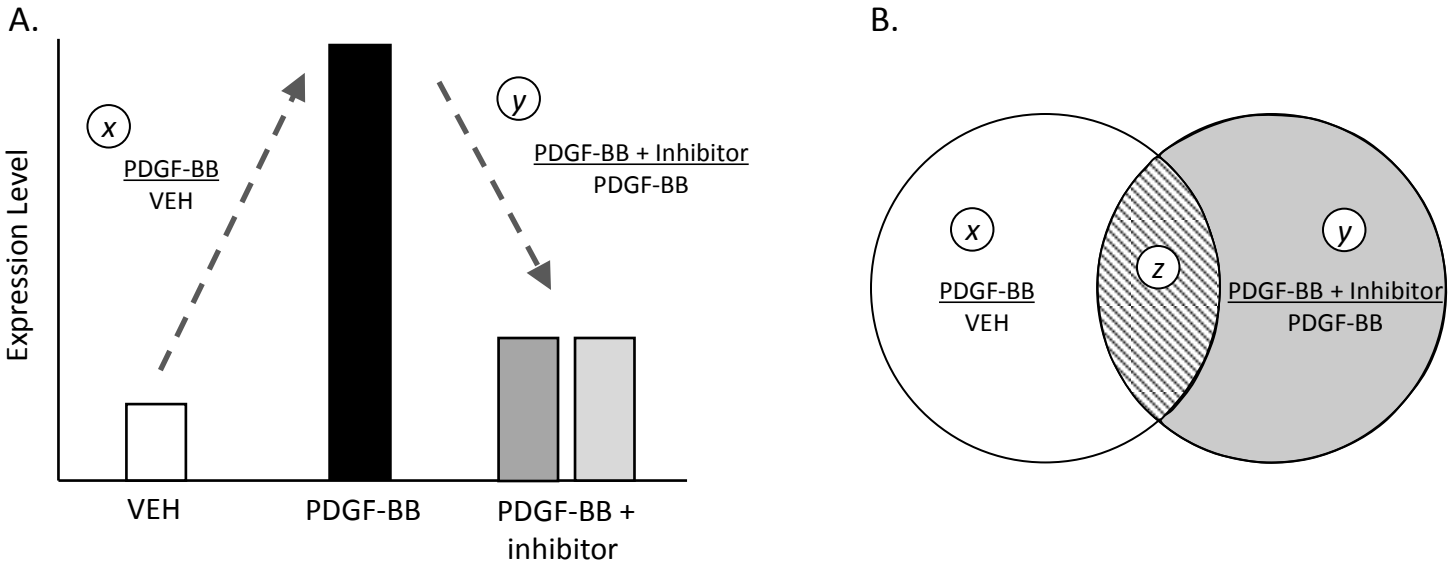

Supplemental Figure III. Identification of Cn/NFAT target genes. Differentially upregulated genes as a result of PDGF-BB treatment were first identified by comparing expression values to those in vehicle treated samples **(A, *x*)**. Secondly, genes exhibiting a reduction in expression as a result of Cn/NFAT inhibition were identified by comparing CsA or A-285222-treated arrays to the PDGF-BB-treated array **(A, *y*)**. Differentially upregulated genes as a result of PDGF-BB treatment **(B, *x*)** were merged with the lists of genes sensitive to Cn/NFAT inhibitors **(B, *y*)** to yield a list of putative PDGF-BB-induced genes dependent on Cn/NFAT activity **(B, *z*)**.

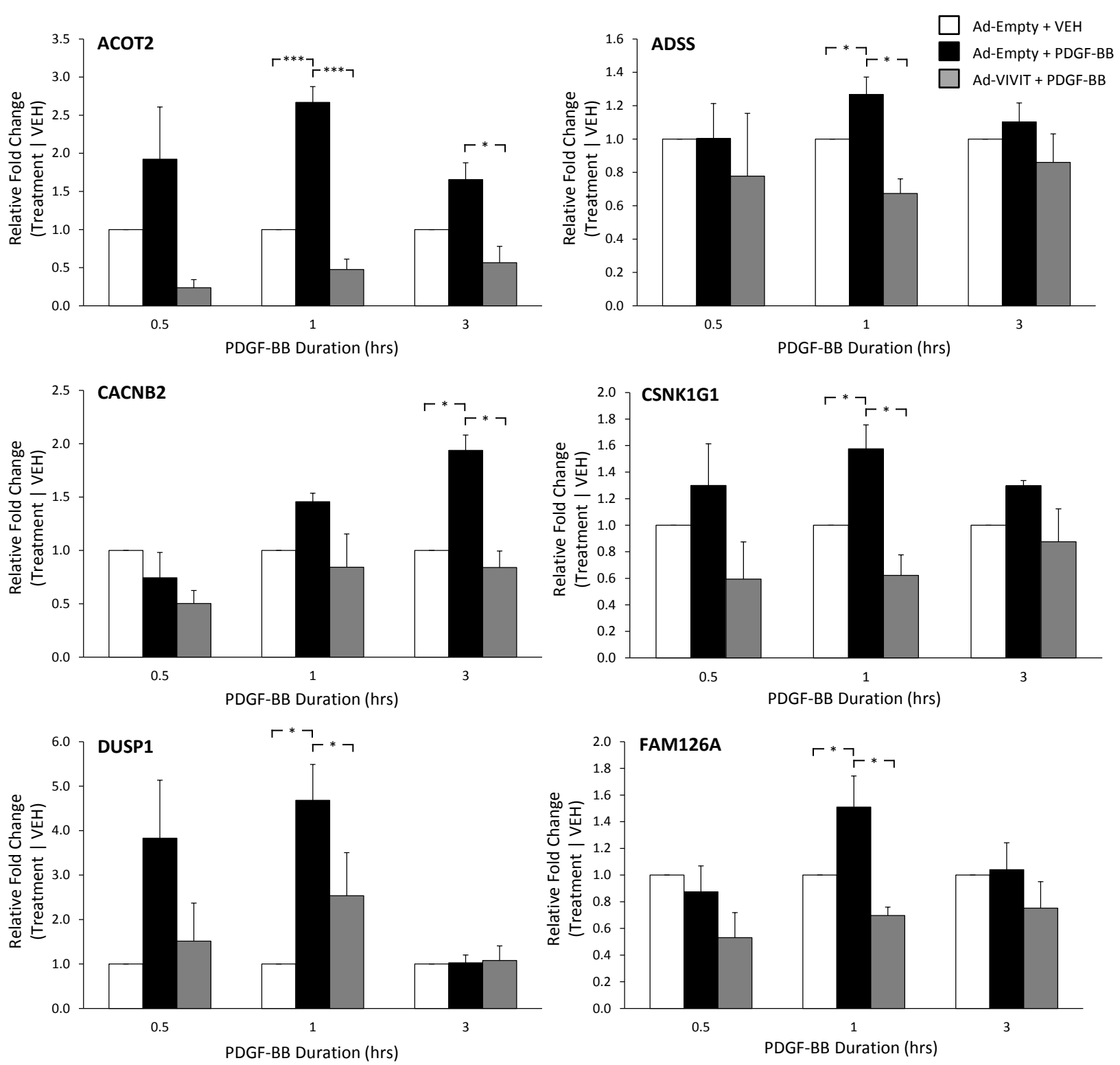

Supplemental Figure IV. Functional NFAT dependency was determined for each putative NFAT target gene through use of VIVIT peptide. mRNA changes reflect relative fold change normalized to vehicle conditions for each time point. mRNA changes are relative to 18s rRNA expression. (n≥3, *p<0.05, ***p<0.001)

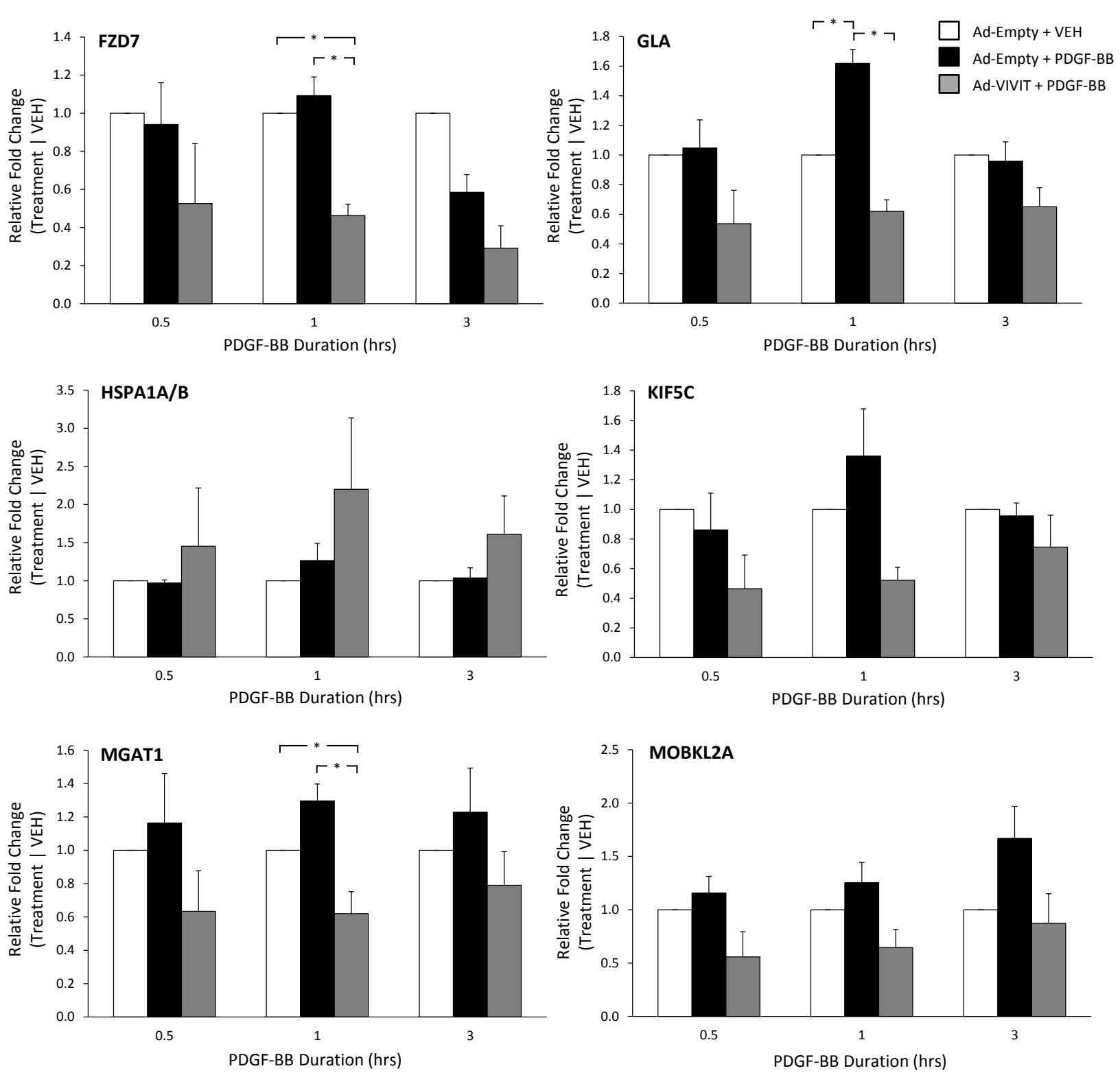

Supplemental Figure IV. Functional NFAT dependency was determined for each putative NFAT target gene through use of VIVIT peptide. mRNA changes reflect relative fold change normalized to vehicle conditions for each time point. mRNA changes are relative to 18s rRNA expression. (n≥3, *p<0.05, ***p<0.001)

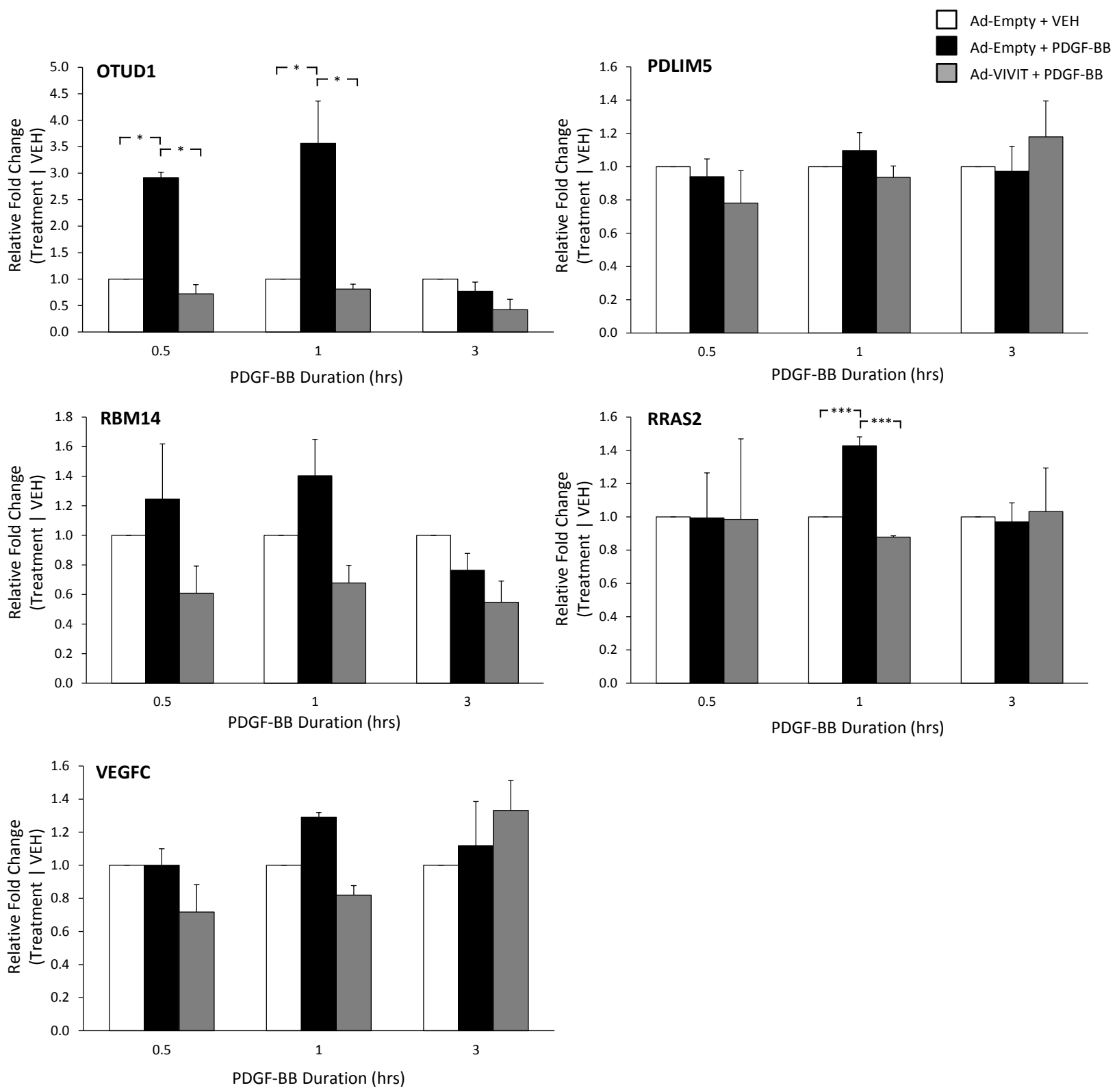

Supplemental Figure IV. Functional NFAT dependency was determined for each putative NFAT target gene through use of VIVIT peptide. mRNA changes reflect relative fold change normalized to vehicle conditions for each time point. mRNA changes are relative to 18s rRNA expression. (n≥3, *p<0.05, ***p<0.001)

ApoE 12wk HFD

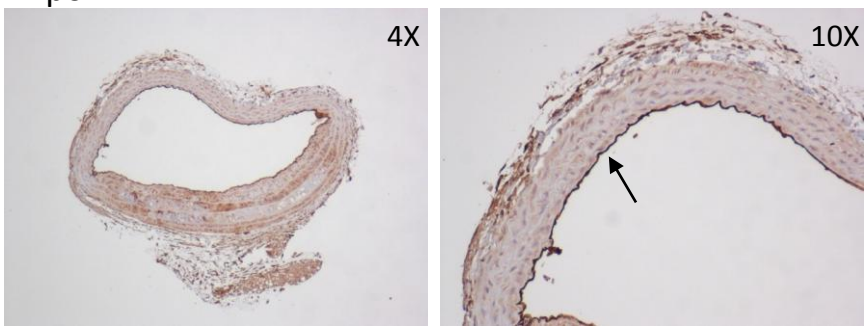

Secondary ONLY

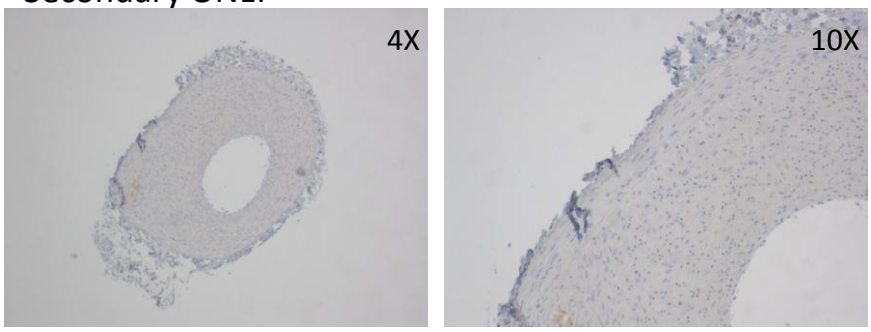

Supplemental Figure V. Immunohistological staining of ApoE$^{-/-}$ mouse aortas show endothelial PROCR expression (arrow). A secondary only control in balloon-injured rat carotid arteries demonstrate minimal non-specific staining.

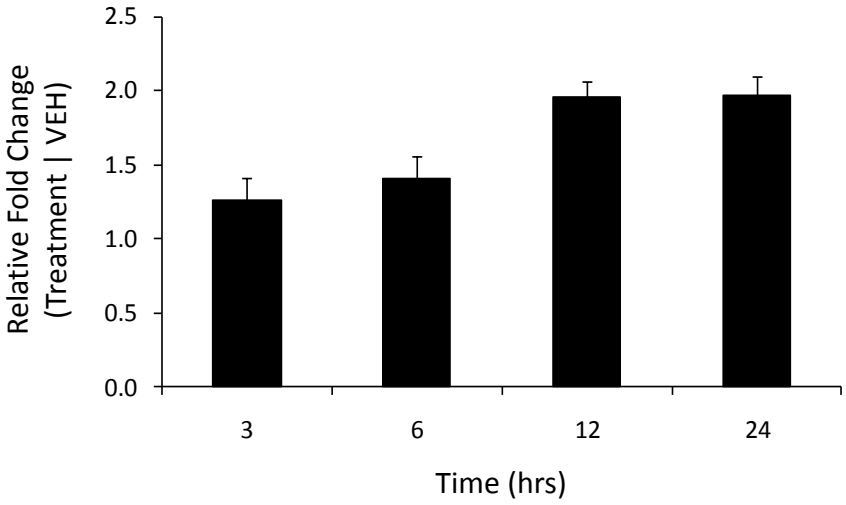

Supplemental Figure VI. Thrombin stimulation induces PROCR promoter activity in RASMCs (n=3). Luciferase output normalized to total protein. Thrombin stimulation at each time point normalized to respective vehicle.